Invited talk at the workshop "Astronomy with Radioactivities" from 29. September to 2. October 1999 in the Ringberg castle, Tegernsee, Germany, editors R. Diehl et al.

Dust Formation in Radioactive Environments

Peter Woitke

Institut für Astronomie und Astrophysik, TU Berlin, Germany,
Sekr. PN 8-1, Hardenbergstraße 36, D–10623 Berlin

Abstract. Basic conditions for the formation of dust grains in stellar environments are summarized. Special emphasis is put upon the proper definition of the "stability" of a dust grain under the prevailing conditions in the ambient medium, including the possibility of thermal non-equilibrium (different dust and gas temperatures) and chemical non-equilibrium in the gas phase. The dust temperatures of pure, crystalline grains with glassy extinction properties (e. g. corundum Al_2O_3, rutile TiO_2 or diamonds) are thereby found to be substantially lower than others (up to 1000 K), which might favor their formation. Additional criteria for dust formation are deduced from the formation of seed particles out of the gas phase (nucleation). Present results of the application of nucleation theory to oxygen-rich gases are reviewed, considering the species $(SiO)_N$, $(MgO)_N$, $(Fe)_N$, Al_xO_y and $(TiO_2)_N$, where only the latter is found to be capable to provide reasonable nucleation rates at high temperatures.

1 Introduction

Dust formation in radioactive environments provides a powerful tool to posthumously analyse the elemental and isotopic composition of astrophysical objects in the laboratory, with a precision unobtainable by spectral observations. The information, e. g. isotopic ratios, is well-recorded in the solid material during the dust formation process. Provided that this information is preserved and unaffected by the residence and the processing in the interstellar medium, the incorporation into the meteorites, and the formation of the Solar System (with the only exception being the internal radioactive decay), very precise informations about various stellar objects can be obtained from the presolar grains found in meteorites (see e. g. reviews by Hoppe and Amari, this conference).

In order to understand and to interpret these data correctly, models for the dust formation process are required which are capable to predict whether and how dust grains are formed in the continuous or explosive outflows of stars. Dust formation is a chemical process and thereby controlled by the local conditions of the ambient medium (gas density and temperature, chemical composition of the gas, local mean radiation intensity). Since these processes are not affected by the isotopic composition of the gas, the question on the origin of such dust grains resembles that of the general origin of the solid phase in space (as e. g. reviewed by Sedlmayr 1994).

2 Stability of dust grains

As a first necessary condition for dust formation, the resulting grains must be thermally stable[1]. The thermal stability of a dust grain is determined by the net effect of chemical reactions taking place *on the surface of the grains*, here for instance on the surface of a corundum grain

$$\mathrm{Al_2O_3(s)} \rightleftharpoons \mathrm{Al_2O_3} \tag{1}$$
$$\mathrm{Al_2O_3(s)} \rightleftharpoons \mathrm{2\,Al + 3\,O} \tag{2}$$
$$\mathrm{2\,H_2 + Al_2O_3(s)} \rightleftharpoons \mathrm{Al_2O + 2\,H_2O}\ , \tag{3}$$

where (s) denotes one unit of the solid which may vaporize into a free molecule (1), may decompose into free atoms (2) or may be transformed by means of a more complex surface chemical

[1] Other non-thermal influences like UV radiation fields, mechanical sputtering etc. may also affect (usually reduce) the dust stability, but it is hard to imagine any formation process if the dust grains are thermally unstable.

reaction (3), also denoted by "chemical sputtering". The reactions directed to the left and to the right will be henceforce called "growth" and "evaporation" reactions, respectively.

For the most simple case of the reaction of type (1), the growth rate (number of growth reactions per second and per unit surface area of the solid) is

$$R_{\rm gr}^{(1)} = n_1 v_{\rm th}(T_{\rm g})\,\alpha(T_{\rm g},T_{\rm d}) \ , \tag{4}$$

where n_1 is the number density of the solid's nominal molecule in the gas phase (the "monomer", here $n_{\rm Al_2O_3}$), $v_{\rm th}$ its thermal velocity and α the sticking probability comprising the available kinetic informations about the surface reaction. $T_{\rm g}$ and $T_{\rm d}$ are the gas and dust temperatures, respectively.

The rate of the reverse (evaporation) reaction in this case is simply the spontaneous evaporation probability $\beta(T_{\rm d})$ per second and per unit area of the solid

$$R_{\rm ev}^{(1)} = \beta(T_{\rm d}) \ . \tag{5}$$

In thermodynamical equilibrium (denoted by $^\circ$), where chemical equilibrium in the gas phase, thermal equilibrium between dust and gas ($T_{\rm g}=T_{\rm d}$) and phase equilibrium ($S=1$, see below) are valid, the growth and evaporation rates are in detailed balance $\mathring{R}_{\rm gr}=\mathring{R}_{\rm ev}$. In this reference state, $\mathring{n}_1$ is equal to $p_{\rm vap}(T_{\rm d})/kT_{\rm d}$, where $p_{\rm vap}$ is the vapor pressure of the monomer. This Milne-type relation can be used to express β

$$\beta(T_{\rm d}) = \frac{p_{\rm vap}(T_{\rm d})}{kT_{\rm d}} v_{\rm th}(T_{\rm d})\,\alpha(T_{\rm d},T_{\rm d}) \ . \tag{6}$$

The net growth rate is hence given by

$$R_{\rm gr}^{(1)} - R_{\rm ev}^{(1)} = R_{\rm gr}^{(1)}\left[1-\frac{p_{\rm vap}(T_{\rm d})}{n_1\,kT_{\rm d}}\,\frac{v_{\rm th}(T_{\rm d})\,\alpha(T_{\rm d},T_{\rm d})}{v_{\rm th}(T_{\rm g})\,\alpha(T_{\rm g},T_{\rm d})}\right] \ . \tag{7}$$

Expanding the last fraction by $n_1^{\rm CE}\,T_{\rm g}\,p_{\rm vap}(T_{\rm g})$, where $n_1^{\rm CE}$ denotes the monomer density in chemical equilibrium in the gas phase *at gas temperature* $T_{\rm g}$ and *according to the actual element abundances in the gas phase* (which may be affected by the consumption by dust formation) yields

$$R_{\rm gr}^{(1)} - R_{\rm ev}^{(1)} = R_{\rm gr}^{(1)}\left[1-\frac{1}{S\;b_{\rm therm}^{(1)}\;b_{\rm chem}^{(1)}}\right] \ , \tag{8}$$

where the following departure coefficients enter into:

$$S = \frac{n_1^{\rm CE}kT_{\rm g}}{p_{\rm vap}(T_{\rm g})} \tag{9}$$

$$b_{\rm therm}^{(1)} = \frac{p_{\rm vap}(T_{\rm g})}{p_{\rm vap}(T_{\rm d})}\sqrt{\frac{T_{\rm d}}{T_{\rm g}}}\;\frac{\alpha(T_{\rm g},T_{\rm d})}{\alpha(T_{\rm d},T_{\rm d})} \tag{10}$$

$$b_{\rm chem}^{(1)} = \frac{n_1}{n_1^{\rm CE}} \ . \tag{11}$$

The supersaturation ratio S expresses the **phase non-equilibrium** between gas and solid and refers to a reference state, where chemical equilibrium in the gas phase and thermal equilibrium ($T_{\rm d}=T_{\rm g}$) holds, $b_{\rm therm}$ corrects for **thermal non-equilibrium** between gas and dust, and $b_{\rm chem}$ accounts for **chemical non-equilibrium** effects in the gas phase.

Patzer et al. (1998a) have shown that a similar expression as Eq. (8) can be obtained for reactions of the general type A(s) + B $\rightleftharpoons$ A$'$(s) + B$'$, e.g. C(s) + H_2 $\rightleftharpoons$ C$'$(s) + C_2H_2, which is important for the growth of carbonaceous dust grains (Gail & Sedlmayr 1988). In this case, the supersaturation ratio S appears with a power equal to the number of monomers $m(i)$ transferred by the reaction (i) and the b-factors are defined in a slightly different way, *but the definition of the supersaturation ratio S remains the same*. It is straightforward to apply the concept described

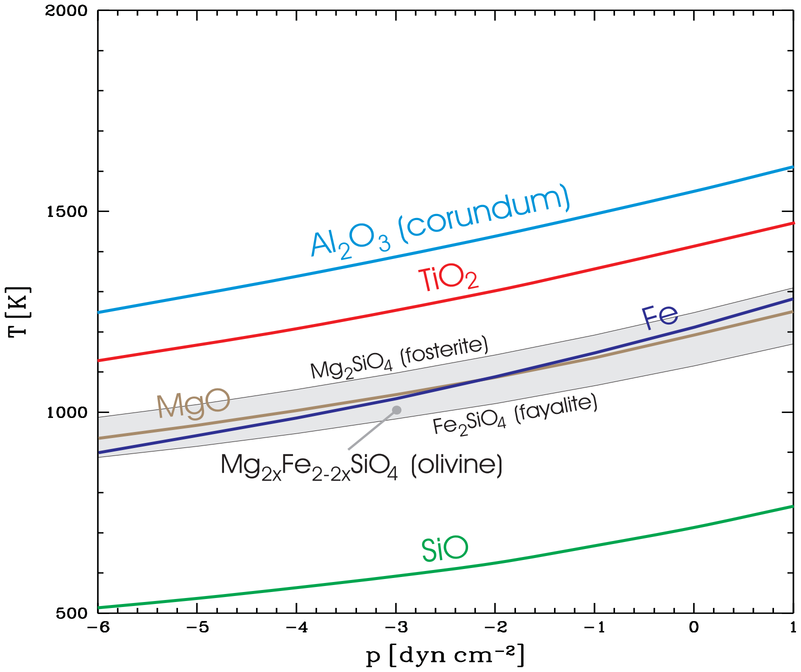

Fig. 1. Sublimation temperatures ($S=1$) of various solid compounds as function of total pressure in a gas with solar element abundances in case of thermal ($b_{\rm therm}=1$) and chemical equilibrium ($b_{\rm chem}=1$). Adopted from Gail & Sedlmayr (1998a, 1999).

above also to the surface reactions of type (2) and (3), if a kinetic description of the forward reaction is at hand. Consequently, the general definition of dust grain stability is given by the following product

$$S^{m(i)}\,b^{(i)}_{\rm therm}\,b^{(i)}_{\rm chem}\begin{cases}<1: \text{net evaporation}\\ =1: \text{stable}\\ >1: \text{net growth}\end{cases} \tag{12}$$

Note that this definition depends on the considered reaction (i). In the case of thermal and chemical equilibrium, however, the stability of the solid is uniquely determined by the supersaturation ratio, meaning that in this case all *possible* surface reactions have the same preferred direction.

The stability limits of several solid compounds in case of thermal and chemical equilibrium ($S=1$) are plotted in Fig. 1. Below such a line the solid compound is stable, above the line it is unstable against vaporization and chemical sputtering. Such calculations lead to the so-called "*dust condensation sequences*"[2]. Following representative cooling trajectories of fixed fluid elements in dust forming objects (henceforth called "cooling flows"), first some rare, but especially tightly bound solid compounds like corundum (Al_2O_3) or rutile (TiO_2) become stable, before the solid materials composed of the more abundant elements Si, Mg and Fe, e. g. olivine ($Mg_{2x}Fe_{2-2x}SiO_4$) bracketed by fosterite (x=1) and fayalite (x=0), reach their stability limits.

2.1 Some remarks on the supersaturation ratio

From thermodynamics, the vapor saturation pressure $p_{\rm vap}$ is obtained by considering the law of mass action for a hypothetical reaction between N monomers and one N-cluster ($N\cdot A_1 \rightleftharpoons A_N$) in the limit $N\to\infty$. The resulting partial pressure of the monomer A_1 in the gas phase is to be identified with $p_{\rm vap}$

$$p_{\rm vap}(T) = p^{\circ}\,\exp\left(\frac{\Delta_{\rm f}^{\circ}G[A({\rm s})] - \Delta_{\rm f}^{\circ}G[A_1]}{RT}\right)\ , \tag{13}$$

[2] A misleading term which confuses stability and formation (see Sect. 3). Such results should rather be denominated by *stability sequences*.

where $p^\varnothing$ is the standard pressure, where the Gibbs free energies of formation $\Delta_{\rm f}^\varnothing G$ refer to, and $\Delta_{\rm f}^\varnothing G[A({\rm s})] = \lim\limits_{N\to\infty} \Delta_{\rm f}^\varnothing G[A_N]/N$ is the Gibbs free energy of one unit in the solid phase.

In cases where the nominal molecule of a solid A is not stable as a free molecule (e. g. fosterite Mg_2SiO_4, pyroxene $Mg_{0.7}Fe_{0.3}SiO_3$ etc.), the definition of the supersaturation ratio (Eq. 9) seems to be problematic at first, because S is given by a fraction of two pressures, which are both virtually zero. Consider, for example, the fictitious species $A = X_xY_y$ composed of two elements X and Y with stoichiometric ratios x and y, respectively. The partial pressure of the corresponding monomer in the gas phase at temperature T in chemical equilibrium is given by the law of mass action

$$p^{\rm CE}_{X_xY_y} = n_1^{\rm CE} kT = \frac{(p_X^{\rm CE})^x (p_Y^{\rm CE})^y}{(p^\varnothing)^{x+y-1}} \exp\left(-\frac{\Delta_{\rm f}^\varnothing G[X_xY_y] - x\Delta_{\rm f}^\varnothing G[X] - y\Delta_{\rm f}^\varnothing G[Y]}{RT}\right) \ . \tag{14}$$

Inserting Eq. (13) and (14) into Eq. (9) shows that *the properties of the monomer cancel out*

$$S(T) = \frac{(p_X^{\rm CE})^x (p_Y^{\rm CE})^y}{(p^\varnothing)^{x+y}} \exp\left(-\frac{\Delta_{\rm f}^\varnothing G[X_xY_y({\rm s})] - x\Delta_{\rm f}^\varnothing G[X] - y\Delta_{\rm f}^\varnothing G[Y]}{RT}\right) \ . \tag{15}$$

Thus, the supersaturation ratio is well-defined, no matter whether the monomer exists in the gas phase or not. Generally speaking, $S > 1$ indicates that it is thermodynamically favorable to convert *any* suitable combination of gaseous species (in chemical equilibrium with each other) into the condensed phase.

The supersaturation ratio is hence completely determined by the Gibbs free energy of formation of the solid compound and the partial pressures of the constituting free atoms (e. g. $p_X^{\rm CE}$, $p_Y^{\rm CE}$) in chemical equilibrium. The latter result from large systems of algebraic equations of type (14) for all gas molecules and ions along with the subsidiary conditions of element and charge conservation (e. g. Tsuji 1973, Gail et al. 1984, Sharp & Huebner 1990, Lodders & Fegley 1995). The results do not only depend on the total gas pressure, but do also depend on the element abundances. For example, Gail & Sedlmayr (1999) have demonstrated that the sublimation temperatures ($S = 1$) of different olivines $Mg_{2x}Fe_{2-2x}SiO_4$ evaporating into vacuum are roughly 200 – 300 K higher than those of the olivines evaporating into a gas with solar element composition, because the free oxygen is partly consumed by the formation of water molecules.

Another example for such dependencies is the well-known "CO-blocking": If C < O, there is almost no free carbon left in the gas phase ($p_{\rm C}^{\rm CE} \to 0$). Consequently, all solids containing carbon are not stable according to Eq. (15). Similarly, in the opposite case C > O, all oxygen-containing solid compounds are unstable. This dependency is generally well-confirmed by observations, but it is strictly valid only in the case of chemical equilibrium. If a certain physical/chemical mechanism can specifically unblock the CO, large $b_{\rm chem}$-factors may occur and the results for the stability of solid compounds can be different. Clayton et al. (1999) argue for carbon dust formation to be possible even in the oxygen-rich ejecta of supernovae explosions, because the CO is partly dissociated by non-thermal electrons from Compton-scattering of γ-rays produced by the radioactivity in the supernova ejecta (see also Clayton, this conference). This scenario seems to be a promising approach to explain the origin of diamond and graphite grains found in presolar meteorites, which were probably formed during supernova explosions as suggested by their isotopic ratios (Amari et al. 1996). However, the temperature-dependence of the stability of the carbon grains under such specific conditions arising from the reverse processes might deserve some additional investigations.

2.2 Thermal non-equilibrium between gas and dust

Deviations between the gas and the dust temperatures can substantially modify the picture of the thermal dust stability outlined above (Fig. 1) and are likely to occur due to the dominating influence of the radiative processes on the internal energy balance of the dust grains (e. g. Gauger et al. 1990). The net radiative heating rate of a single dust grain is given by

$$Q_{\rm rad} = 4\pi \int \pi a^2 Q_{\rm abs}(a,\lambda) \big[J_\lambda - B_\lambda(T_{\rm d})\big] \, d\lambda \ , \tag{16}$$

where $Q_{\rm abs}$ is the absorption efficiency (extinction − scattering) of a spherical dust grain of radius a at wavelength λ, J_λ the local mean radiation intensity, and B_λ the Planck function. The internal energy of the grain, being composed of $\mathcal{N}$ atoms, is given by $E = 3\mathcal{N}kT_{\rm d}$. Accordingly, the temperature change of the grain due to radiative heating and cooling can be expressed by the ordinary differential equation $dy/dt = f(y)$ with $y = T_{\rm d}$ and $f(y) = Q_{\rm rad}(T_{\rm d})/(3\mathcal{N}k)$. For small deviations δy from the stability point $\mathring{y}$, defined by $f(\mathring{y}) = 0$, the change is $dy/dt = f(\mathring{y}+\delta y) \approx f(\mathring{y}) + f'(\mathring{y})\delta y$. The relaxation time scale towards radiative equilibrium is hence $\tau_{\rm rad} = \delta y/(dy/dt) = 1/f'(\mathring{y})$

$$\tau_{\rm rad}^{-1} = \frac{4\pi^2 a^3}{3\mathcal{N}k} \int \frac{Q_{\rm abs}}{a} \frac{\partial B_\lambda(T_{\rm d})}{\partial T_{\rm d}}\, d\lambda \ . \tag{17}$$

In the small particle limit of Mie theory ($\lambda \gg 2\pi a$, e. g. Bohren & Huffman 1983) scattering is negligible ($Q_{\rm abs} \approx Q_{\rm ext}$), and $Q_{\rm ext}/a$ becomes size-independent. Since the first fraction in Eq. (17) is also size-independent, the following simple estimate can be obtained

$$\tau_{\rm rad} \approx \Big(\underbrace{0.002\,{\rm sec}}_{\rm amorph.\,c.} \ldots \underbrace{0.1\,{\rm sec}}_{\rm corundum}\Big) \left(\frac{\rho_{\rm d}}{2\,{\rm g\,cm^{-3}}}\right) \left(\frac{m_0}{20\,{\rm amu}}\right)^{-1} \left(\frac{T_{\rm d}}{1000\,{\rm K}}\right)^{-4} , \tag{18}$$

where the $T_{\rm d}^{-4}$ dependency is strictly valid only for $Q_{\rm abs} \propto 1/\lambda$. $\rho_{\rm d}$ is the mass density of the dust material and m_0 the average mass of one atom in the solid compound. The differences in $\tau_{\rm rad}$ are mainly caused by the different extinction efficiencies ranging from the opaque amorphous carbon to the transparent corundum (see below). Equation (18) states that a typical relaxation towards radiative equilibrium only takes about a few 1/10 s to a few 1/1000 s for small grains, a time which is usually very short compared to other characteristic, e. g. hydrodynamical time scales[3].

Inelastic collisions with the surrounding gas particles generally drive the dust grains towards thermal equilibrium. A part of the impinging gas particles are temporarily adsorbed at the surface of the grains, where they accommodate internal energy before leaving the surface. The respective net collisional energy transfer rate is

$$Q_{\rm coll} = 4\pi a^2\, n_{\rm g} v_{\rm th} \alpha_{\rm acc}\, 2k(T_{\rm g} - T_{\rm d}) \ , \tag{19}$$

where $n_{\rm g}$ is the gas particle density, $v_{\rm th} = \sqrt{kT_{\rm g}/(2\pi m_g)}$ the thermal velocity of the incident gas particles and $\alpha_{\rm acc}$ the thermal accommodation coefficient, which is about 0.15 for uncharged molecular gases at 1000 K (Burke & Hollenbach 1983). The respective collisional time scale is

$$\tau_{\rm coll} \approx 500\,{\rm sec} \left(\frac{\rho_{\rm d}}{2\,{\rm g\,cm^{-3}}}\right) \left(\frac{m_0}{20\,{\rm amu}}\right)^{-1} \left(\frac{a}{0.1\,\mu{\rm m}}\right) \left(\frac{n_{\rm g}}{10^{11}{\rm cm^{-3}}}\right)^{-1} , \tag{20}$$

showing that the collisional energy exchange of the dust grains with the surrounding gas is negligible in comparison to the radiative rates, unless the gas density is as large as $n_{\rm g} \approx 10^{16}{\rm cm^{-3}}$.

Surface chemical reactions may also contribute to the internal energy balance of the grains. Assuming that a growth reaction liberates a formation enthalpy $\Delta_{\rm f}H$ which is completely delivered to the grain, the chemical heating rate is

$$Q_{\rm chem} = 4\pi a^2\, \epsilon\, n_{\rm g} v_{\rm th} \alpha(T_{\rm g}, T_{\rm d})\, \Delta_{\rm f}H \ , \tag{21}$$

where ϵ is the abundance of the condensing species. Assuming $\alpha(T_{\rm g}, T_{\rm d}) = 1$ puts a lower limit to the corresponding characteristical time scale $\tau_{\rm chem} = E/Q_{\rm chem}$

$$\tau_{\rm chem} \approx 7000\,{\rm sec} \left(\frac{\rho_{\rm d}}{2\,{\rm g\,cm^{-3}}}\right) \left(\frac{m_0}{20\,{\rm amu}}\right)^{-1} \left(\frac{a}{0.1\,\mu{\rm m}}\right) \left(\frac{\epsilon\, n_{\rm g}}{10^7{\rm cm^{-3}}}\right)^{-1} \left(\frac{\Delta_{\rm f}H}{10\,{\rm eV}}\right)^{-1} , \tag{22}$$

showing that this mechanism is also negligible under usual conditions. Thus, the internal energy balance of a dust grain is completely controlled by radiative processes and, to a very good degree of accuracy, the dust temperature can be calculated by assuming $Q_{\rm rad} = 0$, which formally results in $T_{\rm d} = T_{\rm d}(J_\lambda, Q_{\rm abs})$.

[3] For larger grains ($\lambda \ll 2\pi a$), the radiative cooling time scale will moderately increase ($\tau_{\rm rad} \propto a$), since large grains absorb energy proportional to their surface area, but store energy according to their volume.

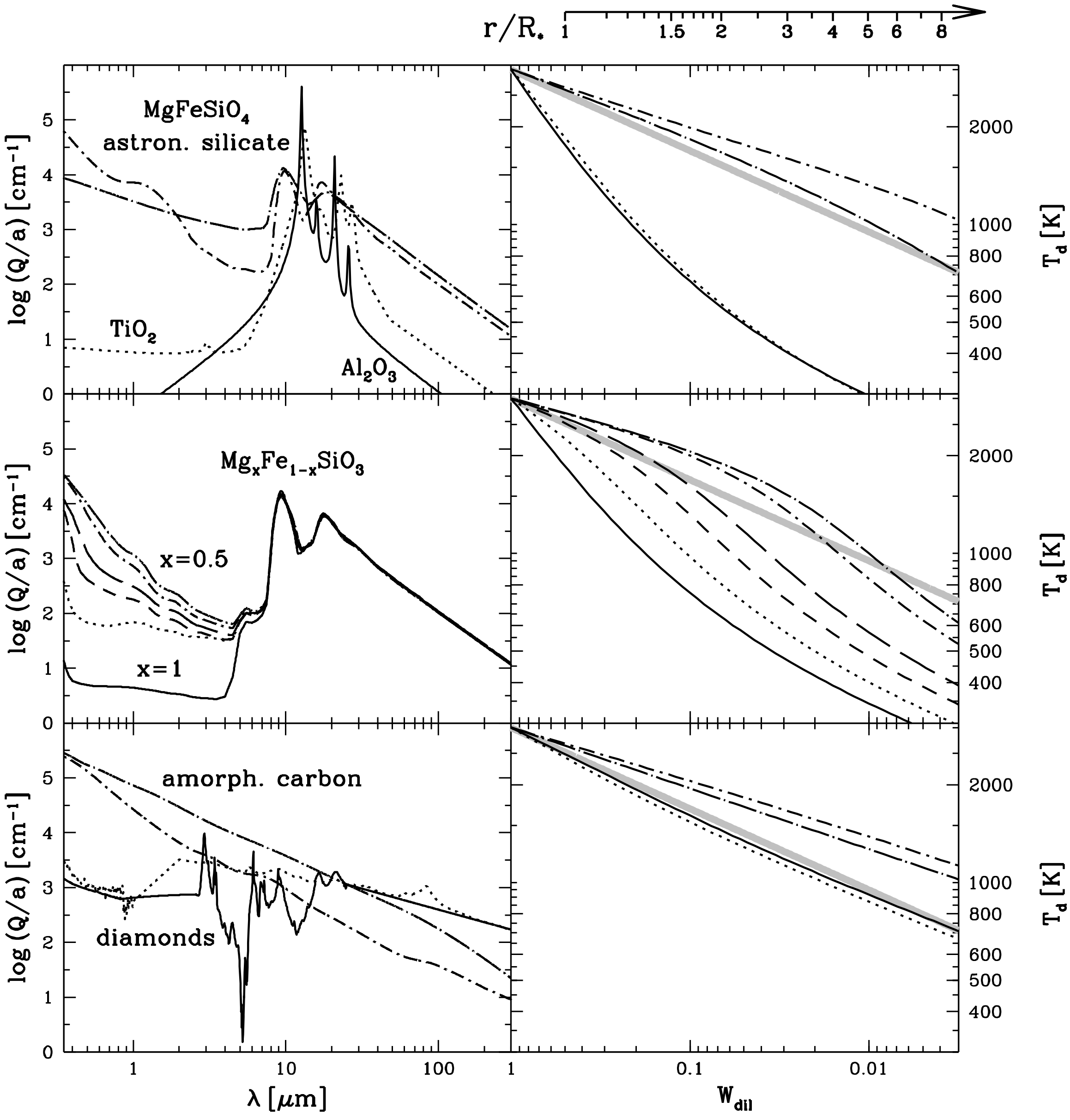

Fig. 2. Extinction efficiencies per dust grain radius $Q_{\rm ext}/a$ of small dust grains (l.h.s.) and calculated dust temperatures (r.h.s.) in a radiation field of type $J_\lambda = W_{\rm dil}\,B_\lambda(3000\,{\rm K})$. The upper axis indicates the corresponding radial distance in units of the stellar radius in the optically thin limit $W_{\rm dil} = 1/2[1 - \sqrt{1-(R_*/r)^2}]$. **First row:** solid line = corundum (Al_2O_3, Posch 1999, priv. comm.), dotted = rutile (TiO_2, Posch 1999, priv. comm.), long dashed–dotted = "astronomical silicate" (Draine 1985), short dashed–dotted = olivine ($MgFeSiO_4$, Dorschner et al. 1995). **Second row:** pyroxenes ($Mg_xFe_{1-x}SiO_3$, Dorschner et al. 1995) with varying iron content x = 1, 0.95, 0.8, 0.7, 0.6, and 0.5. **Third row:** solid line = presolar diamonds (Andersen et al. 1998), dotted = presolar diamonds (Mutschke et al. 1995), long dashed–dotted and short dashed = amorphous carbon dust analogs "cell-1000" and "cell-400", respectively (Jäger 1998). The optical data for the diamonds (Andersen et al. 1998) and the rutile have been extrapolated in the long wavelength region ($\lambda > 25\,\mu$m and $\lambda > 50\,\mu$m, respectively). The thick solid grey line indicates the black body temperature $T_{\rm bb} = W_{\rm dil}^{1/4}\cdot 3000\,{\rm K}$ for comparison.

Figure 2 shows a few examples of calculated dust temperatures for different materials in a radiation field of type $J_\lambda = W_{\rm dil} B_\lambda(T_{\rm eff})$ where $T_{\rm eff} = 3000\,{\rm K}$ has been chosen as a typical value for red giants. Since $T_{\rm d} < T_{\rm eff}$ is always valid, Eq. (16) states that the dust grains are mainly heated in the optical and near IR (where the flux is maximum, here around $1\,\mu$m), whereas cooling occurs mainly in the mid IR (typically around a few μm). For many solid materials, $Q_{\rm ext}$ roughly scales with $1/\lambda$, modified by spectral features (e. g. amorphous carbon, astronomical silicates, see Fig. 2). Such particles are strongly heated and usually hotter than a black body in the prevailing radiation field. However, there also exist so-called "glassy" particles (e. g. corundum Al_2O_3, rutile TiO_2, or the pure enstatite $MgSiO_3$) which are more or less transparent in the optical and near IR, but opaque in the mid IR. Such particles are much less receptive for the incident radiation field and, consequently, much cooler[4,5].

The calculated temperature differences between different solid compounds are found to be as large as 1000 K (see Fig. 2), which demonstrates the importance of thermal non-equilibrium effects for the dust stability sequences and might influence the dust formation process. For example, considering a slight downward temperature deviation of only 200 K ($T_{\rm d} = 900\,{\rm K}$, $T_{\rm g} = 1100\,{\rm K}$), the thermal b-factor defined by Eq. (10) is already as large as $\sim 5{\cdot}10^7$ for a corundum grain. Considering sublimation temperatures of 1350 K, 1200 K and 1050 K for Al_2O_3, TiO_2 and the silicates (compare Fig. 1), small corundum and rutile grains would already be stable at $r \gtrsim 1.05\,{\rm R}_*$ and $r \gtrsim 1.1\,{\rm R}_*$, respectively, in contrast to the silicates which are found to be stable at $r \gtrsim 4.6 - 8.6\,{\rm R}_*$. Similar, but less pronounced results are obtained for presolar diamonds. The dust temperature of small diamonds is found to be about $400 - 600$ K lower than the amorphous carbon dust temperatures. Considering a sublimation temperature of 1750 K for both types of carbon grains, the diamonds get already stable at $r \gtrsim 1.4\,{\rm R}_*$, whereas the stability of the amorphous carbon grains requires $r \gtrsim 2.4\,{\rm R}_*$. This finding might contribute to an explanation of recent detections of diamond signatures in Herbig Ae/Be stars (Guillois et al. 1999). McCabe (1982) reported on similar "inverse greenhouse effects" for SiC grains in contrast to graphite.

Impurities, especially by iron cations, tend to reduce the glassy characteristic of the solids (Henning 1999). For example, an increase of the iron content in pyroxene $Mg_xFe_{1-x}SiO_3$ causes a strong increase of the optical extinction (Dorschner et al. 1995, see Fig. 2). Consequently, the incorporation of impurities does both reduce the thermodynamical stability of the solid material and increase the internal dust temperature. It is not clear whether such dependencies may have a direct influence on the dust formation process itself. Solid annealing and diffusion processes may remove initial misalignments in the lattice and are capable to transport impurities towards the surface, respectively, unless the dust temperature is not too low (Gail & Sedlmayr 1999). Besides the chemical processes acting on the surface of the grains, such processes introduce a certain level of noise also to the inside of the grains and may be regarded as a source of an ongoing structural "mutation". Pushing forward this idea, dust grains incorporating too many impurities would be eliminated by the radiation field and the formation of pure, glassy dust grains might be favored according to the principle "survival of the fittest".

3 Formation of dust grains

The stability of *macroscopic* dust grains discussed so far is a necessary, but not a sufficient condition for dust formation. Figure 3 demonstrates that further conditions for dust formation exist, which must be met by the cooling flow. The figure depicts the results of time-dependent model calculations for the nucleation, growth and evaporation of carbon dust at constant thermodynam-

[4] Larger dust grains are generally less affected by these (inverse) greenhouse effects, because the grains in the large particle limit ($\lambda \ll 2\pi a$) absorb with their geometric cross section which drives the internal dust temperature towards that of a black body.

[5] These results must not be extrapolated to the molecular domain! Clusters and molecules have very different absorption properties and usually cannot be treated in LTE. Therefore, the actual *formation* of such particles (see Sect. 3) is not favored straightforwardly.

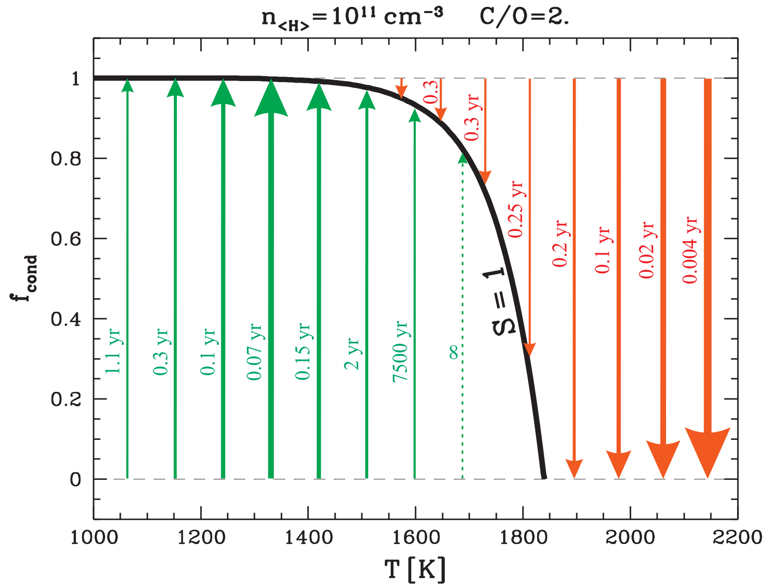

Fig. 3. Dust formation and evaporation time scales in case of thermal and chemical equilibrium in a gas of total hydrogen particle density $n_{<\rm H>}$, solar element abundances and carbon-to-oxygen ratio as indicated. The plotted numbers show the computed values for the times required for the degree of condensation $f_{\rm cond}$ to reach a deviation from its equilibrium value (indicated by the $S=1$–curve) of less than 10% at constant thermodynamical conditions, starting from a dust–free or a fully condensed state where all carbon is present in form of mono–sized grains with $a=1\mu$m, respectively.

ical conditions according to the theories developed by Gail et al. (1984), Gail & Sedlmayr (1988) and Gauger et al. (1990). In this case, of course, the system will relax towards thermodynamical equilibrium for $t\rightarrow\infty$ (including phase equilibrium $S\rightarrow 1$). However, two important aspects shall be mentioned in this context:

- Dust formation is a *slow* process in diluted gases. In order to build up a μm-sized grain, months or years are typically required (depending on the gas density) to pick up sufficient molecules from the gas phase. This time may exceed the hydrodynamical time scales in real cooling flows. *Dust formation requires favorable thermodynamic conditions for a sufficiently long time.*
- The actual formation of a solid body out of the gas phase, where initially no surface sites are present, necessarily starts with the *formation of seed particles*, a process which is well-known to require a large *supersaturation of the gas.* Figure 3 demonstrates that carbon dust formation is impossible at 1700 K and still needs about 7500 years at 1600 K, although the sublimation temperature is about 1850 K in the depicted case. Temperatures as low as 1400 K are required, according to the model, to assure a sufficiently large supersaturation of the gas suitable for nucleation. *Dust formation generally occurs far away from phase-equilibrium.*

3.1 Basics of nucleation theory

Despite its obvious relevance, a reliable description of the nucleation process under astrophysical conditions is still not at hand, especially in the oxygen-rich case[6], where the primary condensates

[6] Research is more advanced in the carbon-rich case, where past research has profited from the large body of experimental data from combustion chemistry, favoring the formation of carbonaceous dust grains via PAH formation (e. g. Keller 1987, Frenklach & Feigelson 1989, Cherchneff et al. 1992, Goeres et al. 1996), but the models still tend to predict much to low formation yields and difficult questions still remain, for example whether or not the hydrocarbon clusters are in thermal equilibrium with the gas.

are basically of heterogeneous type, possibly involving aluminum-, titanium- or zirconium-oxides (Gail & Sedlmayr 1998a). But the identification of the key molecules for the nucleation process is still under discussion, and the limited knowledge of the exact chemical pathway to larger clusters along with the mostly lacking thermodynamical data of the clusters and the reaction rates under extreme low-pressure conditions make any predictions difficult.

Due to these difficulties, former studies have mainly adopted the principles of classical nucleation theory. Basic works in this field are Salpeter (1974), Draine & Salpeter (1977), Yamamoto & Hasegawa (1977), and Gail et al. (1984). In order to shed some light on the nature of the nucleation process, a few key aspects of this theory shall be outlined in the following. A more profound summary can be found e. g. in Gail & Sedlmayr (1998b).

A linear chain of chemical reactions leading from small to large *homogeneous clusters*[7], growing by one monomer per reaction step is considered

$$A_1 \rightleftharpoons A_2 \rightleftharpoons \cdots \rightleftharpoons A_{N-1} \underset{\tau_{\rm ev}^{N}}{\overset{\tau_{\rm gr}^{N-1}}{\rightleftharpoons}} A_N \underset{\tau_{\rm ev}^{N+1}}{\overset{\tau_{\rm gr}^{N}}{\rightleftharpoons}} A_{N+1} \rightleftharpoons \cdots \rightleftharpoons A_{N_{\rm max}} \rightleftharpoons \cdots \quad . \tag{23}$$

The growth and evaporation time scales $\tau_{\rm gr}$ and $\tau_{\rm ev}$ contain the details of the considered growth and evaporation processes and may depend on further particle concentrations involved in the chemical reactions. The concept can be easily extended to multiple growth steps (addition of dimers, trimers and so on). In the following, we restrict ourselves to the case of monomer addition, chemical equilibrium in the gas phase, and thermal equilibrium between clusters and gas particles. A more rigorous treatment can be found in Gail & Sedlmayr (1988) and Patzer et al. (1998a). The evaporation time scales can be expressed by means of the following detailed balance consideration

$$\frac{1}{\tau_{\rm ev}^{N}} = \frac{1}{\tau_{\rm gr}^{N-1}} \frac{\overset{\circ}{f}(N-1)}{\overset{\circ}{f}(N)} \quad . \tag{24}$$

Now, $\overset{\circ}{f}(N)$ denotes an artificial equilibrium cluster size distribution which is obtained by constraining the clusters to be in equilibrium with a supersaturated vapor (Salpeter 1977)[8]

$$\overset{\circ}{f}(N)\, kT = \; p^{\varnothing} \; S^N \exp\left(\frac{N \cdot \Delta_{\rm f}^{\varnothing} G[A(s)] - \Delta_{\rm f}^{\varnothing} G[A_N]}{RT}\right) \; . \tag{25}$$

The basic approach in standard nucleation theory is to consider the reaction network depicted in Eq. (23), truncated to a certain maximum cluster size $N_{\rm max}$, in the stationary limit[9]. The result is the stationary flow of clusters in size space which is identified with the "nucleation rate" J_*, measuring the number of seed particles formed per unit time and volume. By a stepwise elimination procedure of the unknowns $f(N)$, known as Becker-Döring method, it is possible to solve the system of algebraic equations analytically. Assuming $\overset{\circ}{f}(1) = f(1)$, the surprisingly simple result is

$$J_* = \left(\sum_{N=1}^{N_{\rm max}} \frac{\tau_{\rm gr}^{N}}{\overset{\circ}{f}(N)} \right)^{-1} \approx \; \frac{\overset{\circ}{f}(N_*)}{\tau_{\rm gr}^{N_*}} \; . \tag{26}$$

(Gail & Sedlmayr 1988, Köhler et al. 1997). The nucleation rate depends on the growth time scales $\tau_{\rm gr}^{N}$, expressing the efficiency of the growth processes (usually not very temperature-dependent), and on the *equilibrium* cluster distribution $\overset{\circ}{f}(N)$, expressing the strongly temperature-dependent

[7] The clusters A_N are called "homogeneous" when they exactly consist of N monomers, where the monomer can be a free atom or a composite species, e. g. a simple molecule.

[8] This is actually a questionable approach because it requires a "Maxwell demon", who maintains this equilibrium by breaking up the large clusters into monomers and returning them to the gas. An alternative formulation of the problem is given by Patzer et al. (1998a).

[9] In a real dust forming system, the chemical time scales are always substantially smaller than the characteristical (hydrodynamical) residence time scale – otherwise, the nucleation process doesn't work anyway.

efficiency of the reverse processes via Eq. (24). This distribution can be calculated from the Gibbs free energy of the clusters $\Delta_f^{\circ} G[A_N]$ (see Eq. 25) and usually possesses a very pronounced minimum as function of size N. Therefore, the sum in Eq. (26) is mainly determined by a single addend, which is identified with the "critical cluster" and denoted by N_*. Consequently, *the nucleation rate is approximately given by the growth rate of the critical cluster, which is the most unstable cluster along the nucleation path* (see approximate part of Eq. 26)[10].

It is important to note that for the determination of the nucleation rates, the Gibbs free energies of the clusters are absolutely required. Unfortunately, these quantities are mostly unknown because (i) it is difficult to produce these high-temperature clusters in the laboratory and (ii) it is hard to apply *ab initio* theory to larger clusters. Due to these lacking data, the so-called "classical" nucleation theory assumes that the binding defect between N units in the bulk phase and one N-cluster $N \cdot \Delta_f^{\circ} G[A(s)] - \Delta_f^{\circ} G[A_N]$ can be expressed by a "surface tension" times the "surface area" of the clusters (see e. g. Gail et al. 1984). This approach is a matter of debate, because both quantities are not very well-defined at the molecular level (e. g. Donn & Nuth 1985).

In order to put the nucleation theory on a more reliable basis, various attempts have been made to calculate the required cluster properties of astrophysically relevant species. Köhler et al. (1997) and John & Sedlmayr (1997) have calculated such properties for $(MgO)_N$ and $(Fe)_N$ clusters by optimizing the spatial structures of the clusters according to semi-classical potential models. Whereas in the first case, the nucleation rate was found to be completely negligible, the iron-nucleation was found to require $T < 600\,K$. Experimental results on the nucleation of $(SiO)_N$ clusters (Nuth & Donn 1982) led to similar conclusions ($T < 500\,K$).

It was therefore necessary to enlarge the search for the primary condensate in the oxygen-rich case to species containing elements of lower abundance (Gail & Sedlmayr 1998b). By applying density functional theory, Jeong et al. (1999b) obtained the optimized spatial structures and the thermodynamical data of $(TiO_2)_N$ clusters, which were found to be extremely stable with binding energies per nucleus as high as 6 eV. Consequently, a homogeneous nucleation of $(TiO_2)_N$ is possible and leads to considerable nucleation rates already around 1050 K, provided that the cross sections of the strongly exothermal growth reactions $(TiO_2)_N + TiO_2 \rightarrow (TiO_2)_{N+1}$ are close to the geometric cross sections.

Another example are aluminum-oxide clusters, which are of prime interest due to the extreme stability of the corundum bulk phase. Figure 4 shows the results of *ab initio* quantum mechanical calculations for small Al_xO_y clusters with varying stoichiometric ratio (Chang et al. 1998, Patzer et al. 1998b). The binding energies of these clusters are found to be on a much lower level. The most stable clusters are planar molecules with stoichiometric ratio 1:1. Especially the nominal molecule of the corundum, Al_2O_3, is not very stable as a free molecule and virtually not present in the gas phase, meaning that the homogeneous nucleation of $(Al_2O_3)_N$ is impossible, at least very inefficient. The only remaining possibility is therefore a more complex *heterogeneous* nucleation process, where starting from the abundant aluminum bearing species in the gas phase (Al, AlOH, AlO, Al_2O, Al_2O_2), the planar cluster with stoichiometric ratio 1:1 are formed first, before they resemble the 3D-structure of the corundum lattice at much larger cluster sizes. But even then, *an efficient nucleation of aluminum-oxide clusters seems to be not very likely* due to the low stability-level of the small Al_xO_y clusters.

4 Conclusions

This paper has discussed general aspects of the formation of dust grains in astrophysical objects. Special attention has been paid to the *stability* of dust grains under the prevailing conditions of the ambient medium which has been found to depend not only on the local pressure, temperature and element composition of the gas, but also on the radiation field and chemical non-equilibrium effects in the gas phase. Thus, there is no uniform "condensation temperature" of a particular solid

[10] This is also the reason why the choice of $N_{\max}$ is usually not critical as long as its value is suitably larger than N_*.

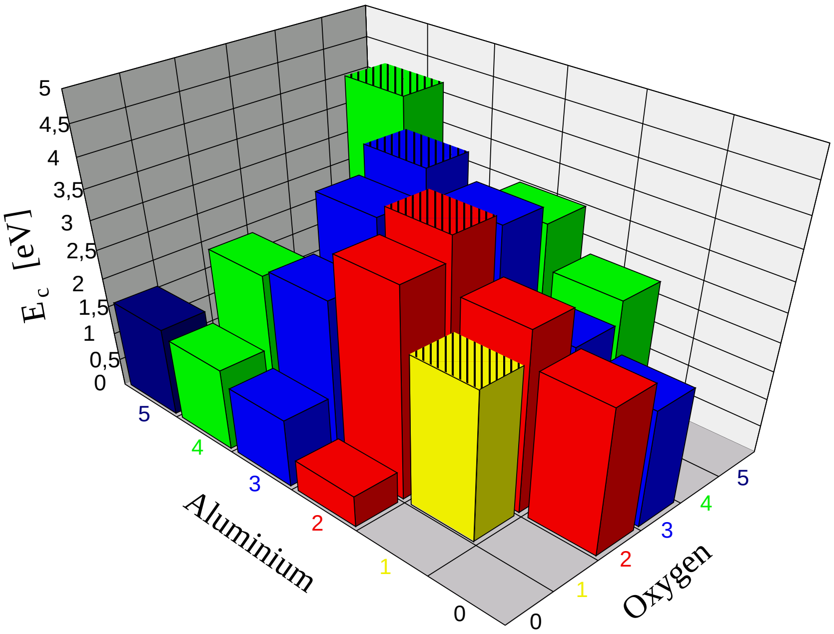

Fig. 4. Binding energies per nucleus for Al_xO_y clusters according to *ab initio* Hartree-Fock and second order Møller-Plesset quantum mechanical calculations with the GAUSSIAN code, basis: 6-31G(d) (Chang et al. 1998, Patzer et al. 1998b).

material as derived from equilibrium condensation models. The main results of this paper can be summarized as follows:

- Due to the strong interaction of the dust grains with the radiation field, thermal non-equilibrium between dust and gas ($T_d \neq T_g$) is a widely expected phenomenon in dust forming objects. This paper has demonstrated that deviations as large as 1000 K can possibly occur. Pure, crystalline dust particles with glassy extinction properties (e.g. Al_2O_3, TiO_2, $MgSiO_3$, diamonds, SiC) are thereby found to be much cooler than others. This effect has important consequences for the stability sequences and possibly favors the formation of such particles in stellar environments.

- Dust formation is a two-step process of nucleation and dust growth. Nucleation requires a large supersaturation of the gas as inferred from the lower stability of small clusters. According to the present knowledge of high-temperature condensates in the oxygen-rich case, nucleation cannot be initiated prior to ~ 1100 K, the best candidate so far being $(TiO_2)_N$ rather than Al_xO_y. At such temperatures, however, the stability of many solid compounds consisting of abundant elements is already warranted. Thus, the forming nuclei are expected to be immediately coated by different solid materials simultaneously, leading to the formation of "dirty", amorphous or poly-crystalline, heterogeneous grains (Jeong et al. 1999a). This straightforward consequence of nucleation theory is, however, in obvious disagreement with the present findings in meteorites, giving direct evidence for the formation of pure, crystalline grains in stellar environments. Furthermore, these particles are found to be rather large (typically a few μm except for the diamonds). The formation of such particles is only expected if all the condensible material grows upon a very few seed particles. Hence, the findings in meteorites point to the existence of a rare, yet unidentified high-temperature condensate in the oxygen-rich case, which may nucleate at considerably higher temperatures.

Acknowledgments: The author would like to thank Dr. Anja Andersen and Thomas Posch for both their contribution in form of optical constants of various solids and their interest and time for discussion on the topic of this paper – even a few days before defense! – and Dr. Beate Patzer for her valuable comments on the manuscript and for providing Fig. 4. This work has been supported by the *DFG, Sonderforschungsbereich 555, Teilprojekt A3.*

References

Amari S., Zinner E., Lewis R. S., 1996, ApJ 470, L101–L104

Andersen A. C., Jørgensen U. G., Nicolaisen F. M., Sørensen P. G., Glejbøl C., 1998, A&A 330, 1080–1090

Bohren C. F., Huffman D. R., 1983, *Absorption and Scattering of Light by Small Particles*, John Wiley & Sons, New York

Burke J. R., Hollenbach D. J., 1983, ApJ 265, 223–234

Chang Ch., Patzer A. B. C., Sedlmayr E., Sülzle D., 1998, Eur. Phys. J. D 2, 57–62

Cherchneff I., Barker J. R., Tielens A. G. G. M., 1992, ApJ 401, 269–287

Clayton D. D., Liu W., Dalgarno A., 1999, Science 283, 1290–1292

Donn B., Nuth J. A., 1985, ApJ 288, 187–190

Dorschner J., Begemann B., Henning T., Jäger C., Mutschke H., 1995, A&A 300, 503–520

Draine B. T., 1985, ApJS 57, 587–594

Draine B. T., Salpeter E. E., 1977, Chem. Phys. 67, 2230–2235

Frenklach M., Feigelson E. D., 1989, ApJ 341, 372–384

Gail H.-P., Keller R., Sedlmayr E., 1984, A&A 133, 320–332

Gail H.-P., Sedlmayr E., 1988, A&A 206, 153–168

Gail H.-P., Sedlmayr E., 1998a, In Sarre P., *Chemistry and physics of molecules and grains in space. Faraday Discussion no. 109*, p. 303, London, GB

Gail H.-P., Sedlmayr E., 1998b, In Hartquist T., Williams D., *The Molecular Astrophysics of Stars and Galaxies*, p. 285, Oxford Science Pub., Oxford, GB

Gail H.-P., Sedlmayr E., 1999, A&A 347, 594–616

Gauger A., Gail H.-P., Sedlmayr E., 1990, A&A 235, 345–361

Goeres A., Keller R., Sedlmayr E., Gail H.-P., 1996, Polycyclic Aromatic Compounds 8, 129–165

Guillois O., Ledoux G., Reynaud C., 1999, ApJ 521, L133–L136

Henning T., 1999, In Le Bertre T., Lèbre A., Waelkens C., *IAU Symp. 191: AGB stars*, p. 221–232, ASP

Jäger C., Mutschke H., Henning T., 1998, A&A 332, 291–299

Jeong K. S., Winters J. M., Sedlmayr E., 1999a, In Le Bertre T., Lèbre A., Waelkens C., *IAU Symp. 191: AGB stars*, p. 233–238, ASP

Jeong K. S., Winters J. M., Sedlmayr E., 1999b, In Hron J., Höfner S., *2nd Austrian ISO Workshop*, p. 37–38, Institute of Astronomy, University of Vienna

John M., Sedlmayr E., 1997, Astrophys. Space Sci. 251(1-2), 219–222

Keller R., 1987, In Léger A., d'Hendecourt L., Boccara N., *Polycyclic Aromatic Hydrocarbons and Astrophysics*, p. 387–397, Reidel Publ. Comp.

Köhler T. M., Gail H.-P., Sedlmayr E., 1997, A&A 320, 553–567

Lodders K., Fegley B., 1995, Meteoritics 30, 661–678

McCabe E. M., 1982, MNRAS 200, 71–82

Mutschke H., Dorschner J., Henning T., Jäger C., Ott U., 1995, ApJ 454, 641–655

Nuth J. A., Donn B., 1982, J. Chem. Phys. 77(5), 2639–2646

Patzer A. B. C., Gauger A., Sedlmayr E., 1998a, A&A 337, 847–858

Patzer A. B. C., Chang, Ch. and John, M. and Sedlmayr, E., 1998b, *IAU Symp. 191: AGB stars*, Poster P3-02, ADS

Salpeter E. E., 1974, ApJ 193, 579–584

Salpeter E. E., 1977, ARA&A 15, 267–293

Sedlmayr E., 1994, In Jørgensen U. G., *IAU Colloquium 146: Molecules in the Stellar Environment*, p. 163–185, Springer–Verlag, Berlin

Sharp C. M., Huebner W. F., 1990, ApJS 72, 417–431

Tsuji T., 1973, A&A 23, 411–431

Yamamoto T, Hasegawa H., 1977, Prog. Theor. Phys. 58(3), 816–828